

Categorization of resistive switching of metal-Pr_{0.7}Ca_{0.3}MnO₃-metal devices

Z. L. Liao, Z. Z. Wang, Y. Meng, Z. Y. Liu, P. Gao et al.

Citation: *Appl. Phys. Lett.* **94**, 253503 (2009); doi: 10.1063/1.3159471

View online: <http://dx.doi.org/10.1063/1.3159471>

View Table of Contents: <http://apl.aip.org/resource/1/APPLAB/v94/i25>

Published by the AIP Publishing LLC.

Additional information on *Appl. Phys. Lett.*

Journal Homepage: <http://apl.aip.org/>

Journal Information: http://apl.aip.org/about/about_the_journal

Top downloads: http://apl.aip.org/features/most_downloaded

Information for Authors: <http://apl.aip.org/authors>

ADVERTISEMENT



Categorization of resistive switching of metal-Pr_{0.7}Ca_{0.3}MnO₃-metal devices

Z. L. Liao, Z. Z. Wang, Y. Meng, Z. Y. Liu, P. Gao, J. L. Gang, H. W. Zhao, X. J. Liang, X. D. Bai, and D. M. Chen^{a)}

Beijing National Laboratory for Condensed Matter Physics, Institute of Physics, Chinese Academy of Sciences, Beijing 100190, People's Republic of China

(Received 28 March 2009; accepted 14 May 2009; published online 24 June 2009)

Resistive switching (RS) characteristics of a Pr_{0.7}Ca_{0.3}MnO₃ (PCMO) film sandwiched between a Pt bottom electrode and top electrodes (TE) made of various metals are found to belong to two categories. Devices with TE made of Al, Ti, and Ta exhibit a large *I-V* hysteresis loop and bipolar RS, but those with TE made of Pt, Ag, Au, and Cu do not. Transmission electron microscopy reveals that a thin metal-oxide layer formed at the interface between the former group of TE and PCMO, but not for the latter group of TE. Analysis shows that the categorization depends on the Gibbs free energy of oxidation of the TEs with respect to that of PCMO. © 2009 American Institute of Physics. [DOI: 10.1063/1.3159471]

Resistance switching (RS) in metal oxides has drawn growing interest¹⁻⁶ because of its potential applications in high-performance nonvolatile resistance random access memory devices. There are two types of RS. One is unipolar RS (URS) such as NiO, TiO₂, and other binary transition metal oxides (TMO),^{1,2} whereby SET, switching from a high resistance state (HRS) to a low resistance state (LRS), and RESET, switching from LRS to HRS, occur at different biases of the same polarity, either positive or negative. The other type of RS is bipolar like some perovskite materials, whereby SET and RESET occur at the opposite bias polarity.⁵ Several mechanisms have been proposed to account for these two types of RS.⁷⁻¹⁰ Electric field induced filament formation and rupture by Joule heating is thought to be the most likely explanation for the URS. The origin for the bipolar RS (BRS) remains elusive despite a significant increase in experimental findings in the past year. Indeed, recent reports have shown diverse effects of the metal electrodes on the RS as the electrode material can participate in oxidation/reduction process,¹¹ or in trapping and detrapping of the oxygen vacancies.¹² The role played by metal contacts in these devices goes beyond the Schottky contacts as in typical semiconductor devices, and may very well hold the key to the successful engineering of practical devices.

Here, we report a remarkable trend found in the RS characteristics of Pr_{0.7}Ca_{0.3}MnO₃ (PCMO) films sandwiched between a Pt bottom electrode (BE) and top electrodes (TE) made of various metals. Devices with TE made of Al, Ti, and Ta are found to exhibit a large current-voltage (*I-V*) hysteresis loop and BRS, but those with TE made of Pt, Ag, Au, and Cu do not. High-resolution transmission electron microscopy (HRTEM) reveals that a thin metal-oxide layer formed at the interface between the former group of TE and PCMO but not for the latter group of TE. Interestingly, the analysis shows that the *I-V* characteristics strongly depend on the Gibbs free energy of oxidation of the TEs but have no correlation to TE's work function. The distinct *I-V* characteristics of these two groups can be attributed to the presence/

absence of the metal oxide layer and a solid state oxidation/reduction process facilitated by a localized electrical field.

The PCMO film was fabricated on a 170 nm Pt buffer layer on a silicon wafer by a special low temperature (<400 °C) back-biased face-target-sputtering process.¹³ X-ray diffraction (XRD) θ - 2θ profile of the film confirmed that the PCMO film is *c*-axis oriented, and HRTEM images revealed that the PCMO film is polycrystalline and is 125 nm thick. To form sandwiched devices, we fabricated an array of 100 μm^2 electrodes of a number of materials, 30 nm thick and with a 600 μm separation in *x* and *y* directions, on top of the PCMO by magnetron sputtering. The schematic of the device cross-section and measurement setup is shown in Fig. 1(a). *I-V* characterizations and pulse switching were carried out with Keithley 2400 and Agilent 81110A, respectively. The data presented below was collected with a typical loop of bias sweep, 0 \rightarrow + V_{max} \rightarrow 0 \rightarrow - V_{max} \rightarrow 0, unless indicated otherwise. Devices with TE made of Al, Ti, and Ta show stable RS under 50 ns and 5 V drive pulses. As an example, Fig. 1(b) illustrates the pulse generated RS of a Ti TE device.

Figure 2 shows the *I-V* characteristics of seven different TEs on PCMO/Pt. Quite noticeably, large hysteresis loops at negative bias were present for Al/PCMO/Pt [Fig. 2(b)], Ti/PCMO/Pt [Fig. 2(c)], and Ta/PCMO/Pt [Fig. 2(d)], while almost no hysteresis was observed in Ag (Pt, Au, Cu)/PCMO/Pt devices [Fig. 2(a)]. The *I-V* loop labeled "F" in Figs. 2(b)–2(d) is the "forming process," i.e., when a voltage is applied to the virgin state of a device and ramped above a

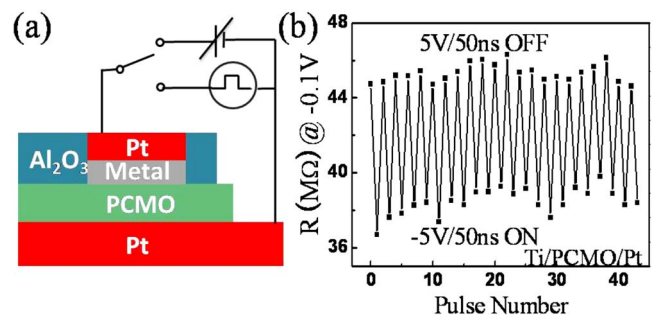


FIG. 1. (Color online) (a) Schematic of devices and the measurement setup. (b). Resistance switching under pulsed cycles for a Ti/PCMO/Pt device.

^{a)} Author to whom correspondence should be addressed. Tel.: 86-10-82648158. FAX: 86-10-82640266. Electronic mail: dmchen@aphy.iphy.ac.cn.

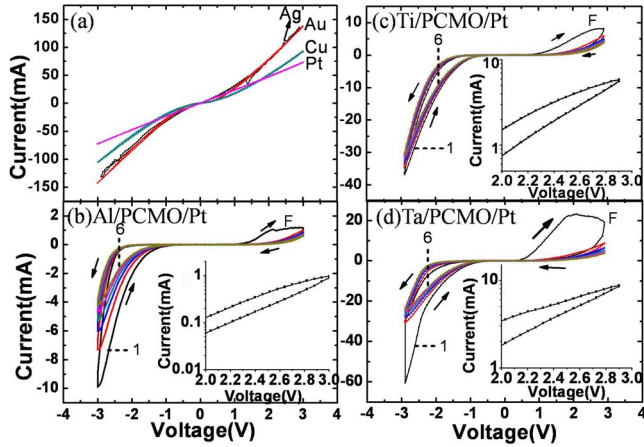


FIG. 2. (Color online) I - V characteristics for (a) Ag, Cu, Au, Pt/PCMO/Pt, (b) Al/PCMO/Pt, (c) Ti/PCMO/Pt, and (d) Ta/PCMO/Pt. The data was taken with bias looped from 0 V \rightarrow 3 V \rightarrow -3 V \rightarrow 0 V. There are six consecutive loops for (b), (c), and (d), and label-1 marks the first loop, and six is the last. The size of the loop reduces progressively from one to six. Label-F marks the forming process. Inset of (b), (c), or (d) shows the blow up of the hysteresis loop at positive bias.

threshold (1.8–2.5 V), resulting in a new physical state that exhibits hysteresis subsequently. There are six consecutive loops for each specimen [Figs. 2(b)–2(d)] and some degrees of fatigue of the size of the hysteresis loop (reducing from 1 to 6) can be seen. However, after multiple bias sweeps, the I - V characteristics and the hysteresis become repeatable. Quite interestingly, all devices made with nonreactive metal (Pt, Ag, Au, and Cu) TEs do not display a similar “forming” and hysteresis characteristics. Note that the resistance of Pt/PCMO/Pt device is only 43 Ω , indicating very low Pt/PCMO contact and PCMO bulk resistance. In addition, the Pt/PCMO/Pt device does not show RS under I - V sweep up to ± 3 V. Thus, the Pt BE should have a negligent effect on the overall measurement and data taken from devices made with other TEs should primarily reflect the effect of the TE materials.

Prior to the forming process, the I - V characteristics in a small bias region below the threshold of all the devices are reversible regardless the TE material. The virgin resistance (VR) is a good measure of the contact resistance between the TE and PCMO. Figure 3(a) plots the VR against the work function of the TE material where the work function of PCMO (4.89 eV) is also marked.¹⁷ Note that there is essentially no direct correlation between the TE’s work function and the VR. On the other hand, VR for nonreactive-metal/

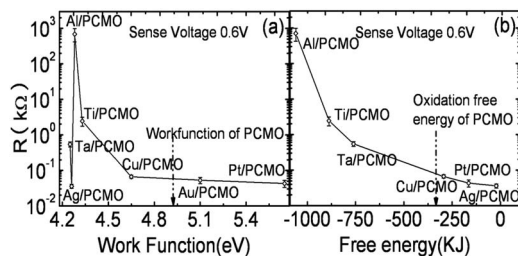


FIG. 3. (a) VR vs work function. The data of each TE material is an average over 100 devices, and small error bars indicate that these devices are quite uniform. The dashed line marks the work function of PCMO. (b) VR vs metal-oxide formation free energy taken from Refs. 14 and 15. The dashed line at -366 kJ/mol. indicates the oxidation free energy of PCMO from Ref. 16.

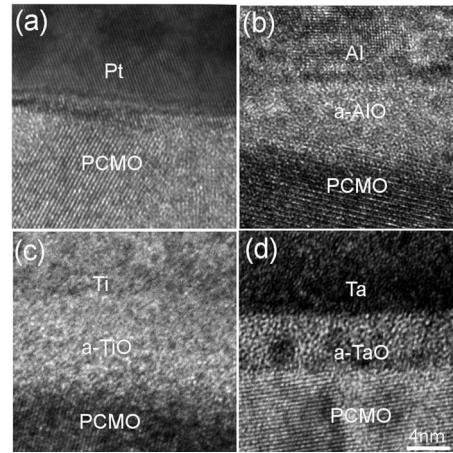


FIG. 4. HRTEM images of interfaces between top electrodes and PCMO. (a) Pt/PCMO, (b) Al/PCMO, (c) Ti/PCMO, and (d) Ta/PCMO. All figures have the same scale shown in (d).

PCMO/Pt is much less than VR of (Al, Ti, Ta)/PCMO/Pt. These observations suggest that the interface is not a typical Schottky barrier formed by charge redistribution at the interface. For example, there is a large work function difference between Ag and PCMO (4.26 versus 4.89 eV) but Ag/PCMO/Pt has a very low VR and linear I - V .

To elucidate the above observations, HRTEM images of top interfaces of as-prepared samples of (Pt, Al, Ti, Ta)/PCMO were taken and are shown in Figs. 4(a)–4(d). An amorphous layer was found in between (Al, Ti, Ta) and PCMO, but not in Pt/PCMO interface, or (Ag, Au, Cu)/PCMO interface (images not shown). Amorphous oxide layers at (Ta, Ti)/PCMO interfaces have also been confirmed using electron energy loss spectroscopy in two recent reports.^{18,19} The relative high VR is somehow associated with the presence of the interfacial metal oxide. Figure 3(b) plots VR versus the oxidation free energy of the TE material. It shows that the VR decreases with increasing oxidation free energies of TEs. Note that the oxidation free energy of PCMO falls between these two groups. Thus upon deposition, oxidation of the TE and reduction of PCMO at the interface will occur spontaneously for the active metal group (Al, Ti, Ta), but not for the nonreactive metal group (Pt, Ag, Au, or Cu), resulting in dramatically different interfaces for the two groups.

To date, experimental findings on how various metal contacts on PCMO affect RS in a sandwiched-structure have yet to converge. Tsubouchi *et al.*²⁰ have surveyed a combination of TE1/PCMO/TE2 where TE1, TE2 are Mg, Ag, Al, Ti, Au, Ni, and Pt, and concluded that only electrode pairs including at least one Al showed RS. Kawano and co-workers,^{18,19} however, have found that both Ta/PCMO/Pt and Ti/PCMO/Pt exhibit bipolar RS with the former switching faster due to a thinner oxide layer. Sawa *et al.*⁸ studied TE/PCMO/SrRuO₃/PCMO/TE devices (TE being Pt, Au, Ag and Ti) and found that only device with Ti electrode shows RS.

Combining these reports and the present results, we found quite remarkably that the TEs of the PCMO devices can be categorized into two groups, the nonreactive metal group versus the reactive metal group, simply based on the relative oxidation free energy with respect to PCMO. They show dramatically different I - V and RS characteristics. It

should be noted that there are reports that show RS in Ag/PCMO/Pt devices but with a reversed polarity of SET and RESET voltage compared with devices of reactive metal TE,²¹ and hence do not contradict to the above categorization.

Binary TMO sandwiched between two metal electrodes typically display URS.^{1,2} More recently, Jeong *et al.*³ have discovered BRS for a Pt/TiO₂/Pt device by using a forming process at a lower current compliance (<0.1 mA), and attributed the BRS to an electrochemical reaction mechanism to contrast the filamentary model for the URS. For TE/PCMO/Pt devices where the TE is a metal in the reactive group, only BRS has been reported to date, suggesting that the oxide layer and the oxygen deficient PCMO region both play the critical roles. Resistivity for bulk PCMO is 10⁻¹ to 10⁻² Ω cm (Ref. 22) while that for a thin film PCMO is 10³–10⁴ Ω cm due to lower oxygen concentration.⁸ Our Pt/PCMO/Pt device shows a resistivity of ~3.4 × 10² Ω cm. The resistivity of the LRS of the devices with reactive group TEs is also on the same order (see Fig. 2). This implies that the resistance of the oxide layer at LRS is rather small, but becomes dominant at HRS. Oxygen vacancies in TiO₂ are known to be *n*-type dopants, V_O²⁺, which transform a stoichiometric TiO₂ from insulating into semiconducting.²³ The device as fabricated has abundant V_O²⁺ in the TiO_{2-x} layer at the Ti/PCMO interface [Fig. 4(c)] and hence its VR is in LRS. A positive voltage applied to the TE will drive the V_O²⁺ in the Ti-oxide toward PCMO layer and oxidation of Ti-oxide region causes the switching to HRS. When a negative bias is applied to TE, most of the applied voltage will then drop across the oxide layer resulting in a large local electrical field which attracts V_O²⁺ from PCMO toward Ti-oxide, and the reduction of the Ti oxide layer causes a switching back to the LRS. The fatigue on the hysteresis loops shown in Figs. 2(b)–2(d) hence reflects the imbalance between oxidation and reduction during the initial cycles of switching. The migration of the highly mobile oxygen ion in and out of the very thin (~5 nm) metal oxide layer results in a very short switching time of 50 ns [Fig. 1(b)].

The above model can be extended to devices made with other TE in the reactive metal group. While these TEs can be readily oxidized at room temperature (RT) so long as the oxygen ion migration is facilitated by the electrical field, reduction of TEs at RT, however, may need further assistance of local Joule heating to overcome the energy barrier for disassociation. For a given SET voltage, the degrees of reduction of the TEs [Figs. 3(b)–3(d)] are inversely scaled to the Gibbs free energy of Fig. 3(b).^{14–16} During the SET and RESET, the oxygen deficient region of the PCMO acts as a reservoir for storing and supplying oxygen ions. Although the resistivity of PCMO also changes as the oxygen concentration varies, it is much smaller than the change of resistance in the oxide layer. For devices made with TE in the nonreactive metal group, the absence of the metal oxide layer can explain why no appreciable *I*-*V* hysteresis are observed, even though oxygen vacancies may still be shuffled between TE and BE and some degrees of oxidation/reduction at the opposite side of the PCMO may still occur. Sawa *et al.*⁸ have proposed that SET and RESET create two levels of defect states at the interface which trap different amount

of charges and hence create two types of Schottky barriers. The drawback of this model is its inability to naturally account for the categorization of the electrode materials shown above.

In conclusion, we have shown that the contacting material of the TE in a TE/PCMO/Pt thin-film device plays a critical role in determining the device *I*-*V* characteristics. In particular, we have found that metal-PCMO-Pt devices can be categorized into two groups based on whether the Gibbs free energy for oxidation of the TE is greater or less than PCMO oxidation free energy. This unique property of metal-PCMO-metal device could be exploited for novel applications.

We thank 4DS Inc. for supplying the PCMO films and invaluable discussions. This work is supported in part by Chinese Academy of Sciences (Grant No. KJCX2-SW-W26), National Science Foundation of China (Grant No. 90406017), and by Ministry of Science and Technology of China (Grant Nos. 2007CB925002 and 2008AA031401).

- ¹S. Seo, M. J. Lee, D. H. Seo, E. J. Jeoung, D.-S. Suh, Y. S. Joung, I. K. Yoo, I. R. Hwang, S. H. Kim, I. S. Byun, J.-S. Kim, J. S. Choi, and B. H. Park, *Appl. Phys. Lett.* **85**, 5655 (2004).
- ²B. J. Choi, D. S. Jeong, S. K. Kim, C. Rohde, S. Choi, J. H. Oh, H. J. Kim, C. S. Hwang, K. Szot, R. Waser, B. Reichenberg, and S. Tiedke, *J. Appl. Phys.* **98**, 033715 (2005).
- ³D. S. Jeong, H. Schroeder, and R. Waser, *Electrochem. Solid-State Lett.* **10**, G51 (2007).
- ⁴X. Wu, P. Zhou, J. Li, L. Y. Chen, H. B. Lv, Y. Y. Lin, and T. A. Tang, *Appl. Phys. Lett.* **90**, 183507 (2007).
- ⁵M. Hamaguchi, K. Aoyama, S. Asanuma, Y. Uesu, and T. Katsufuji, *Appl. Phys. Lett.* **88**, 142508 (2006).
- ⁶S. Q. Liu, N. J. Wu, and A. Ignatiev, *Appl. Phys. Lett.* **76**, 2749 (2000).
- ⁷D. S. Shang, Q. Wang, L. D. Chen, R. Dong, X. M. Li, and W. Q. Zhang, *Phys. Rev. B* **73**, 245427 (2006).
- ⁸A. Sawa, T. Fujii, M. Kawasaki, and Y. Tokura, *Appl. Phys. Lett.* **85**, 4073 (2004).
- ⁹I. H. Inoue, S. Yasuda, H. Akinaga, and H. Takagi, *Phys. Rev. B* **77**, 035105 (2008).
- ¹⁰C. Yoshida, K. Kinoshita, T. Yamasaki, and Y. Sugiyama, *Appl. Phys. Lett.* **93**, 042106 (2008).
- ¹¹C. B. Lee, B.S. Kang, A. Benayad, M. J. Lee, S.-E. Ahn, K. H. Kim, G. Stefanovich, Y. Park, and I. K. Yoo, *Appl. Phys. Lett.* **93**, 042115 (2008).
- ¹²M. Hasan, R. Dong, H. J. Choi, D. S. Lee, D.-J. Seong, M. B. Pyun, and H. Hwang, *Appl. Phys. Lett.* **93**, 052908 (2008).
- ¹³M. Nagashima and D. Schmidt, U.S. Patent No. 6,962,648 (8 November 2005); Z. Z. Wang, Z. L. Liao, and D. M. Chen (unpublished).
- ¹⁴H.-G. Lee, *Chemical Thermodynamics for Metals and Materials* (Imperial College, London, 1999), pp. 127–130.
- ¹⁵G. V. Samsonov, *The Oxide Handbook*, 2nd ed. (IFI/Plenum, New York, 1982), pp. 44–48.
- ¹⁶S. Shirasaki, H. Yamamura, H. Haneda, K. Kakegawa, and J. Mouri, *J. Chem. Phys.* **73**, 4640 (1980).
- ¹⁷D. W. Reagor, S. Y. Lee, Y. Li, and Q. X. Jia, *J. Appl. Phys.* **95**, 7971 (2004).
- ¹⁸H. Kawano, K. Shono, T. Yokota, and M. Gomi, *Appl. Phys. Express* **1**, 101901 (2008).
- ¹⁹K. Shono, H. Kawano, T. Yokota, and M. Gomi, *Appl. Phys. Express* **1**, 055002 (2008).
- ²⁰K. Tsubouchi, I. Ohkubo, H. Kumigashira, M. Oshima, Y. Matsumoto, K. Itaka, T. Ohnishi, M. Lippmaa, and H. Koinuma, *Adv. Mater. (Weinheim, Ger.)* **19**, 1711 (2007).
- ²¹A. Odagawa, H. Sato, I. H. Inoue, H. Akoh, M. Kawasaki, Y. Tokura, T. Kanno, and H. Adachi, *Phys. Rev. B* **70**, 224403 (2004).
- ²²Y. Tomioka, A. Asamitsu, H. Kuwahara, Y. Moritomo, and Y. Tokura, *Phys. Rev. B* **53**, R1689 (1996).
- ²³P. Knauth and H. L. Tuller, *J. Appl. Phys.* **85**, 897 (1999).